IEEE Photonics Journal
An IEEE Photonics Society Publication

Open Access

Broadband IF-Over-Fiber Transmission With Parallel IM/PM Transmitter Overcoming Dispersion-Induced RF Power Fading for High-Capacity Mobile Fronthaul Links

Volume 10, Number 1, February 2018

Shota Ishimura
Byung Gon Kim
Kazuki Tanaka
Kosuke Nishimura
Hoon Kim, ***Senior Member, IEEE***
Yun C. Chung, ***Fellow, IEEE***
Masatoshi Suzuki, ***Fellow, IEEE***

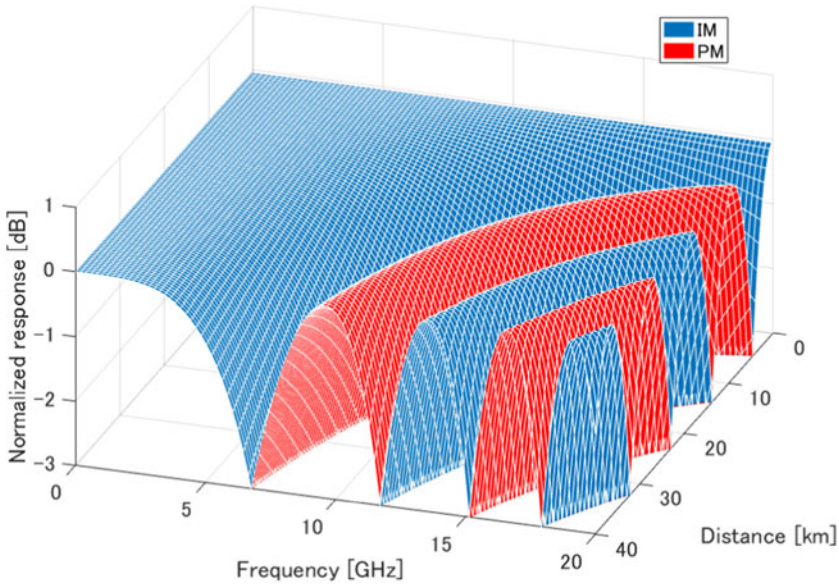

DOI: 10.1109/JPHOT.2017.2787722
1943-0655 © 2017 IEEE

IEEE photonics SOCIETY

IEEE

Broadband IF-Over-Fiber Transmission With Parallel IM/PM Transmitter Overcoming Dispersion-Induced RF Power Fading for High-Capacity Mobile Fronthaul Links

Shota Ishimura,[1,2] **Byung Gon Kim**,[1,2] **Kazuki Tanaka**,[1,2] **Kosuke Nishimura**,[1,2] **Hoon Kim**,[1,2] ***Senior Member, IEEE***, **Yun C. Chung**,[1,2] ***Fellow, IEEE***, **and Masatoshi Suzuki**,[1,2] ***Fellow, IEEE***

[1]KDDI Research, Inc., Fujimino-shi 356-8502, Japan
[2]School of Electrical Engineering, KAIST, Daejeon 34141, South Korea

DOI:10.1109/JPHOT.2017.2787722

Manuscript received December 4, 2017; revised December 15, 2017; accepted December 22, 2017. Date of publication January 1, 2018; date of current version January 17, 2018. Corresponding author: Shota Ishimura (e-mail: sh-ishimura@kddi-research.jp).

Abstract: We demonstrate a broadband and long-distance intermediate frequency-over-fiber (IFoF) transmission scheme employing a transmitter composed of parallel intensity/phase (IM/PM) modulators with appropriate bandwidth allocations to IM and PM. Due to the proposed scheme, we can eliminate all the null frequencies caused by dispersion-induced RF power fading, which, in turn, enables us to significantly increase the available bandwidth. In addition, our system does not require any synchronization between IM and PM, which reduces complexity compared to conventional parallel transmitter architecture. We successfully transmitted 20 $\times$ 360 MHz filtered orthogonal-frequency-division-multiplexed signals corresponding to a common public radio interface equivalent data rate of 524.28 Gbps over a 30- and 40-km single-mode fiber satisfying the 8% threshold for the error-vector magnitude values for all the subcarriers. These results show that our proposed IFoF transmission scheme is scalable to long-distance mobile fronthaul links for 5G and beyond.

Index Terms: Centralized RAN (C-RAN), mobile fronthaul, IF-over-fiber, dispersion-induced RF power fading.

1. Introduction

To date, optical access technology has been developed mainly to provide wired consumer access services such as fiber-to-the-home or fiber-to-the-curb in combination with feeder lines such as coaxial cable (i.e., hybrid fiber-coaxial) or metallic wireline (i.e., very-high-bit-rate digital subscriber line). However, due to the acceleration in the speed of wireless access, the number of subscribers to wired access services has begun to approach a growth plateau, whereas that of wireless access services continues to grow constantly. Of course, to provide high-speed mobile services, wired (optical) access lines are indispensable. Considering such a trend, in the next decade, optical access transmission technology has to evolve so as to realize convergence with wireless transmission systems at a higher level than ever before. In particular, such an evolution will be particularly vital

for mobile fronthaul links accommodating the wireless signals for the 5th generation (5G) or beyond in centralized radio access network (C-RAN) architecture.

C-RAN already has been introduced with high-level coordination technologies such as enhanced inter-cell interference coordination (eICIC) and coordinated multi-point (CoMP) transmission and reception in LTE-A systems [1]. Current C-RAN mainly employs Common Public Radio Interface (CPRI) for the mobile fronthaul links between baseband units (BBUs) located at central offices and remote radio heads (RRHs) located at antenna sites. However, CPRI is based on digital transmission of baseband signals that convey quantized waveforms of in-phase and quadrature (IQ) signals [2]. Such a transmission scheme is so-called "digital radio-over-fiber (D-RoF)", and it is known that the required data rate of CPRI is about sixteen times that of the user data rate as a typical value. Considering the continuous growth in the user data rate per base station, which is assumed to be 20 Gbps at maximum in 5G, it is apparent that D-RoF is not scalable in 5G or beyond. Several approaches to solve this issue are now being widely discussed, and one possible way is to change the splitting point between functions of BBU and RRH. In the technical report produced by the 3rd Generation Partnership Project (3GPP) [3], eight options are defined for the functional split. It is known that high-layer splits up to option 6 have high bandwidth utilization efficiency since additional headers are relatively small [4]; however, their centralized control ability is significantly weakened. On the other hand, low-layer splits such as option 7 have good centralized control ability, while sacrificing the bandwidth utilization efficiency. Therefore, functional splits have trade-off relations between bandwidth utilization efficiency and centralized control ability.

Another approach is to employ frequency-division multiplexing (FDM) with an analog RoF transmission scheme, which is intermediate frequency-over-fiber (IFoF). IFoF corresponds to option 8 (CPRI); however, it has a much higher bandwidth utilization efficiency because delivered wireless signals are directly converted from the electrical to the optical domain. In addition, it can maintain perfect centralized control because only the RF part is in the distributed unit like CPRI. Thus, IFoF has the potential to overcome the trade-off relations.

Since the IFoF transmission scheme has attracted much attention, several papers have been reported recently as described below. By using an LTE signal having a bandwidth of 20 MHz or an LTE-A signal having a bandwidth of up to 100 MHz, IFoF transmission has been demonstrated; [5] reported transmission of 48 $\times$ 20-MHz signals over a 5-km single-mode fiber (SMF) and [6] 128 $\times$ 100-MHz signals over a 20-km SMF focusing on massive multiple-input and multiple-output (MIMO) with a sub-Nyquist sampling technique. As for an IFoF transmission experiment using signals having a bandwidth exceeding 100 MHz, targeting 5G and beyond, transmission of 32 $\times$ 200-MHz signals over a 1-km SMF has been demonstrated [7]. However, high-capacity IFoF transmission through long-distance SMF is yet to be reported, because dispersion-induced RF power fading severely degrades performance of double-sideband (DSB) signals in such conditions due to the destructive interference between the upper and lower sideband [8].

One of the approaches to overcome the RF power fading is the optical single sideband (OSSB) technique. However, especially for wideband signals, additional digital signal processing (DSP) including the Hilbert transform [9], [10] or optical filtering [11] is required, which will increase the system's complexity and reduce flexibility. Another approach based on DSB modulation is utilizing phase modulation to intensity modulation (PM-IM) conversion through fiber transmission [12]–[14]. [12] achieves power fading compensation by adjusting the state of polarization (SOP) before the polarizer. However, such an SOP manipulation has to be done manually and the system is still complicated. On the other hand, [13], [14] introduce a modulation-diversity or parallel-transmitter architecture employing both IM and PM. Taking advantage of the complementary relationship between IM and PM response, the transmitter can compensate for fading to some extent. However, the paths between IM and PM should be carefully adjusted to make the response flat, which results in high complexity in the transmitter. Further, in all these references, no experiments using a broadband signal such as multiple aggregated 5G signals with IFoF technology have been reported.

In [15], we have proposed the transmitter architecture with a parallel IM/PM transmitter along with the scenario of simultaneous transmission of microwave and millimeter-wave signals. In this paper, applying the parallel IM/PM transmitter to an IFoF system, we experimentally demonstrate a

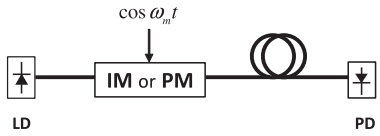

Fig. 1. Analytical model for frequency response of an intensity or phase modulated signal through an optical fiber.

broadband and long-distance IFoF transmission. We assign multiple IF signals to IM or PM independently with appropriate bandwidth allocations based on measured IM and PM responses, which requires no synchronization between IM and PM and significantly reduces transmitter complexity compared to the cases in [13], [14]. Furthermore when the bandwidth allocation process is automatically programmed, it offers us flexible solutions without dependence on transmission distance. In the experiment, filtered orthogonal-frequency-division-multiplexed (f-OFDM) signals of 20 $\times$ 360-MHz corresponding to wireless throughput of about 30 Gbps were generated by the parallel transmitter with appropriate bandwidth allocations to IM and PM, and were transmitted over a 30-km and 40-km SMF in a single wavelength channel. If the same signal is transmitted by CPRI, the required transmission capacity reaches 524.28 Gbps (= 20 $\times$ 2 $\times$ 16 $\times$ 614.4 $\times$ 16/15 $\times$ 10/8 Mbps). We measured error-vector magnitudes (EVMs) of all the channels at all the transmission distances, and confirmed that all the values satisfy the 8% EVM requirement of 64-QAM OFDM signals specified in 3GPP [16].

The organization of this paper is as follows: In Section 2, we review the frequency response of the IM and PM signal in direct-detection (DD) systems and show the complementary relation between them. In Section 3, we describe the principle of the parallel IM/PM transmitter. Section 4 provides the experimental results of a broadband IFoF transmission. Finally, we conclude this paper in Section 5.

2. Response of IM/PM-DD Links

In this section, we review the analysis of the frequency response of IM and PM signals over a dispersive optical link as already described in [17], [18]. The analytical model is shown in Fig. 1. A single tone RF signal $\cos \omega_m t$ is optically modulated by IM or PM. First, we consider the IM signal response. Here, we assume IM has almost zero chirp. The normalized optical field modulated by IM can be written as

$$E_{IM}(t) = \sqrt{1 + m_i \cos \omega_m t} \exp(j\omega_0 t), \tag{1}$$

where ω_0 is the angular frequency of the optical carrier and m_i is the intensity modulation index. When the modulation index is small, the IM optical field can be approximated as

$$\begin{aligned} E_{IM}(t) &\approx (1 + m_i \cos \omega_m t) \exp(j\omega_0 t) \\ &= \exp(j\omega_0 t) + \frac{m_i}{2}\{\exp[j(\omega_0 + \omega_m)t] + \exp[j(\omega_0 - \omega_m)t]\}. \end{aligned} \tag{2}$$

On the other hand, the transfer function of a dispersive optical link is given as

$$H = \exp\left[-j\frac{D\lambda^2 L}{4\pi c}\omega_m^2\right], \tag{3}$$

where D is the dispersion parameter, λ is the wavelength of the optical carrier, L is the length of the fiber, and c is the speed of the light. The optical field after fiber transmission is derived from (2)

and (3) as

$$E_{IM}(t) = \exp(j\omega_0 t) + \frac{m_i}{2}\left\{\exp\left[j(\omega_0+\omega_m)t - \frac{D\lambda^2 L}{4\pi c}\omega_m^2\right] + \exp\left[j(\omega_0-\omega_m)t - \frac{D\lambda^2 L}{4\pi c}\omega_m^2\right]\right\}. \quad (4)$$

An electrical output signal from a photodiode (PD) is proportional to the intensity of the optical field, i.e.,

$$i(t) \propto |E(t)|^2. \quad (5)$$

Substituting (4) into (5), the electrical output consisting of DC components, desired ω_m components and undesired second-order $2\omega_m$ components can be derived. When the modulation index is small enough, the second-order component is negligible. Thus, ignoring the DC component, the output can be approximately given as

$$i(t)_{IM} \approx 2m_i \cos\left(\frac{D\lambda^2 L}{4\pi c}\omega_m^2\right)\cos\omega_m t. \quad (6)$$

From the result, the normalized power response of the IM signal as a function of ω_m is given as

$$P_{IM}(\omega_m) \approx \cos^2\left(\frac{D\lambda^2 L}{4\pi c}\omega_m^2\right). \quad (7)$$

The IM response has periodic null points causing dispersion-induced RF power fading.

Next, we consider the response of the PM signal. The optical field modulated by PM can be approximately given as

$$E_{PM}(t) = \exp(j\omega_0 t) + j\frac{m_p}{2}\left\{\exp[j(\omega_0+\omega_m)t] + \exp[j(\omega_0-\omega_m)t]\right\}. \quad (8)$$

where m_p is the phase modulation index. As in the case of IM, the PM optical field after fiber transmission can be derived from (3) and (8) as

$$E_{PM}(t) = \exp(j\omega_0 t) + j\frac{m_p}{2}\left\{\exp\left[j(\omega_0+\omega_m)t - \frac{D\lambda^2 L}{4\pi c}\omega_m^2\right] + \exp\left[j(\omega_0-\omega_m)t - \frac{D\lambda^2 L}{4\pi c}\omega_m^2\right]\right\}. \quad (9)$$

Substituting (9) into (5) and selecting the fundamental frequency components, the output signal from PD can be approximately given as

$$i(t)_{PM} \approx 2m_i \sin\left(-\frac{D\lambda^2 L}{4\pi c}\omega_m^2\right)\cos\omega_m t. \quad (10)$$

Thus, the normalized power response of the PM signal as a function of ω_m can be obtained as

$$P_{PM}(\omega_m) \approx \sin^2\left(\frac{D\lambda^2 L}{4\pi c}\omega_m^2\right). \quad (11)$$

It is obvious that the IM and PM responses [(7) and (11)] have a complementary relationship and when either IM or PM is null at a certain frequency, the other one reaches a maximum point at the frequency. This means even in the frequency range where dispersion-induced RF power fading degrades IM signal quality, PM signal can cover the frequency range instead of IM. Fig. 2(a) shows the 3-dB bandwidth of the IM response as a function of frequency and distance. As the distance or frequency increases, the available bandwidth shrinks. On the other hand, Fig. 2(b) shows the

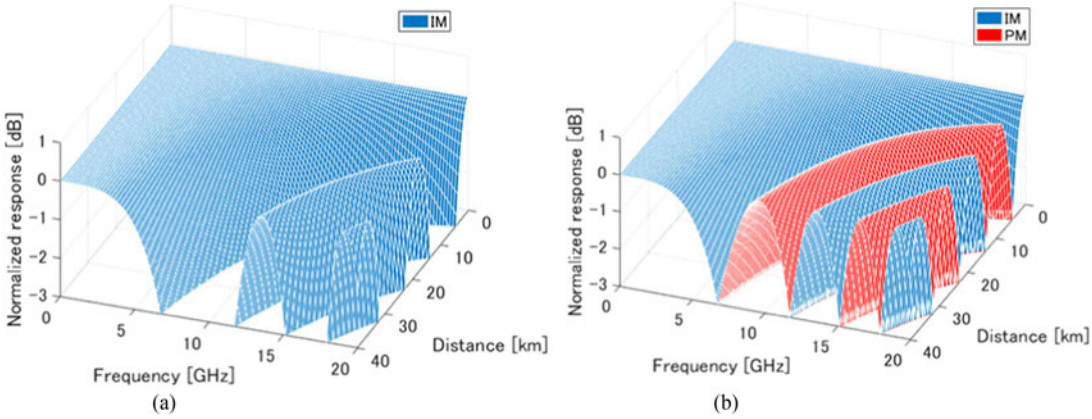

Fig. 2. 3-dB responses as a function of frequency and distance. (a) Case of IM alone. (b) Case of IM and PM.

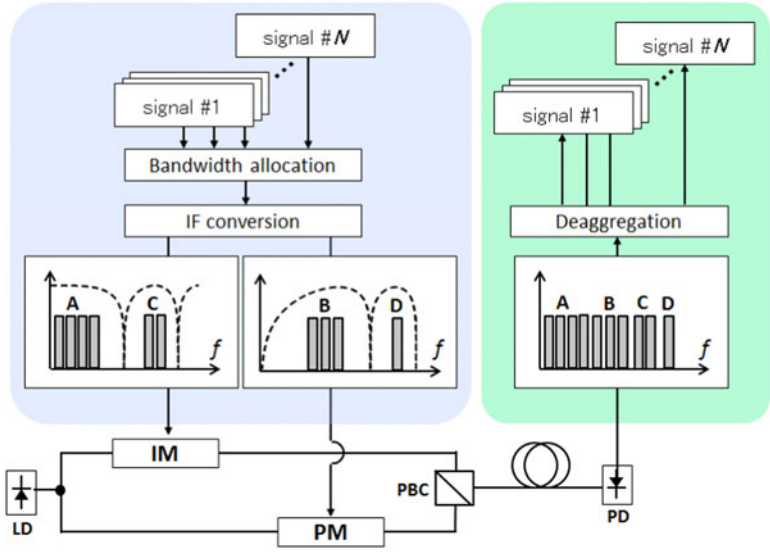

Fig. 3. Conceptual diagram of the parallel IM/PM transmission system.

IM response together with the PM response. It is found that PM can effectively compensate for the frequency ranges which IM cannot cover alone.

3. Principle of Proposed Parallel IM/PM Transmission System

By taking advantage of the complementary relation between the IM and PM response, we propose an IFoF transmission system employing a parallel IM/PM transmitter with appropriate bandwidth allocations, which can overcome dispersion-induced RF fading.

Fig. 3 shows a conceptual diagram of the system with the parallel transmitter. After the generation of multiple signals which will be aggregated on the IF band, the bandwidth allocation block decides which modulator should be used for each signal based on frequency responses of IM and PM to avoid their null points. For example, signals on bands B and D in Fig. 3 are located around the null frequencies if they are assigned to IM. On the other hand, PM has maximum responses around the two bands. Thus, the block decides to assign the signals on bands B and D to PM. Prior to transmission, we have to know the frequency responses of IM and PM. In order to know the responses, we can send test signals to measure them. A similar technique for frequency response

measurement is employed in optical discrete multi-tone (DMT) transmission system for allocating proper QAM format to each frequency component. Alternatively, if the dispersion parameter and fiber length are known, we can simply predict the responses from (7) and (11) without sending the test signals. Subsequently, we assign IF channels either to IM or PM based on the responses. Once it is decided, the measurement and bandwidth assignment are not necessary unless the fiber length or the number of the IF channels is changed.

In the band assignment process, guard bands between IM and PM are not always necessary because as shown in Fig. 3(b), there are almost no gaps between the 3-dB responses of IM and PM. After deciding the frequency allocations, each signal is upconverted to the IF band and sent to IM or PM. Optical IM and PM signals are multiplexed on orthogonal *x*- and *y*-polarizations by a polarization beam combiner (PBC) to avoid the interference between IM and PM. At the receiver, only one PD is needed because the PM signal is effectively converted to the IM signal after fiber transmission.

Thanks to the parallel transmitter and the bandwidth allocations, we can transmit broadband signals without being affected by RF power fading. Of course, this system requires PM, a 3-dB coupler and PBC in addition to IM. However, if we use a dual-electrode Mach-Zehnder modulator (DEMZM) instead of the bulky IM/PM transmitter, we can avoid the insertion of such additional devices. For example, if one of the two inputs to DEMZM has the same amplitude with an opposite polarity, we can get an IM signal, which is referred to as "push-pull operation," while if it has the same amplitude with the same polarity, we can get a PM signal. Therefore, by changing the polarity of one of the two ports for each IF signal, we can selectively generate an IM/PM band with only one MZM. Compared to other RF power fading compensation techniques such as SSB generation, this proposed system is much simpler. For example, if SSB generation is done by DSP, the Hilbert transform is necessary to get a signal having 90 degree phase shifts in all frequency components. When the signal has a large bandwidth, implementing DSP to perform the Hilbert transform is not easy. On the other hand, in the proposed system, even if the bandwidth is large, the required process to avoid RF power fading is only selection of IM or PM for each IF channel prior to transmission without relying on such a sophisticated DSP, which significantly reduces complexity compared to SSB generation. In addition, since each IF signal is perfectly independent of each other, no synchronization between them is required. In the scheme described in [14], time delay between IM and PM has to be carefully adjusted. If the lengths of the paths are not optimal, the frequency response is still affected by RF power fading. On the other hand, in the proposed system, we do not need to be concerned about the time delay, which reduces complexity in the transmitter compared to conventional schemes proposed in [13], [14].

4. Experiment and Results

To verify the aforementioned concept, we demonstrated the transmission of 20 $\times$ 360-MHz f-OFDM signals over a 30-km and 40-km SMF. The experimental setup is shown in Fig. 4. f-OFDM, obtained by signal filtering with a finite impulse response (FIR) filter, is a waveform proposed for the 5G mobile system to mitigate out-of-band emissions and support different service scenarios [20]. First, we generated 20 OFDM signals with an IFFT/FFT size of 2048 points. Each OFDM signal consists of 1000 subcarriers with 64-QAM-modulated symbols and 200 subcarriers with pilots. The subcarrier spacing was set at 300 kHz. Thus the baseband sampling rate was 614.4 MHz. Subsequently, we added 7% cyclic prefix (CP) to the signal and sent it to the FIR filter based on a Hamming window function with 1024 taps to generate an f-OFDM signal having a bandwidth of 360 MHz. After generating f-OFDM signals, they were multiplexed in the IF band based on the frequency response of IM and PM. Thanks to the reduction of out-of-band emissions by the filtering process, we can multiplex the signals with a narrow channel spacing. For example, in our experiment, the guard band between IF signals was set at 3 MHz which corresponds to 1% of one IF bandwidth.

Prior to the signal transmission, the frequency response of IM and PM for each transmission distance was measured. Fig. 5(a) and (b) shows the response of IM and PM in the case of both 30-km and 40-km transmission, respectively. The 3-dB bandwidths of IM for 30-km and 40-km were

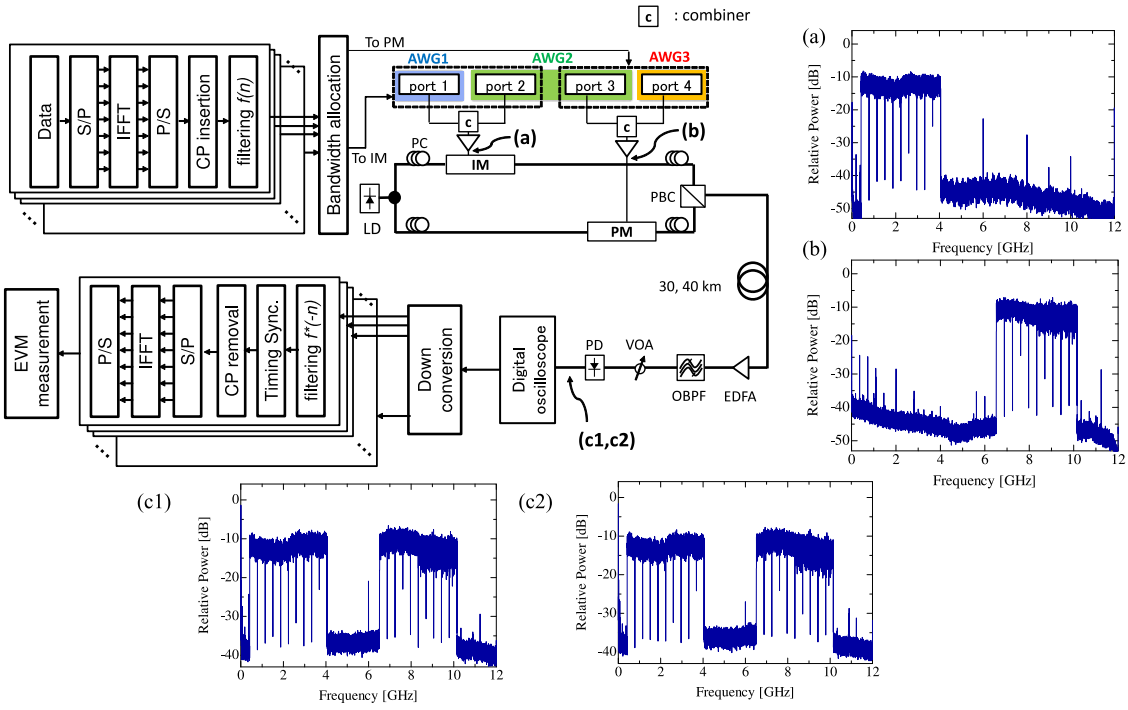

Fig. 4. Experimental setup for the parallel IM/PM transmission system with the electrical spectrum at each point. (a) and (b)Spectrum before driving IM or PM, respectively. (c1) and (c2) After 30-km and 40-km transmission, respectively.

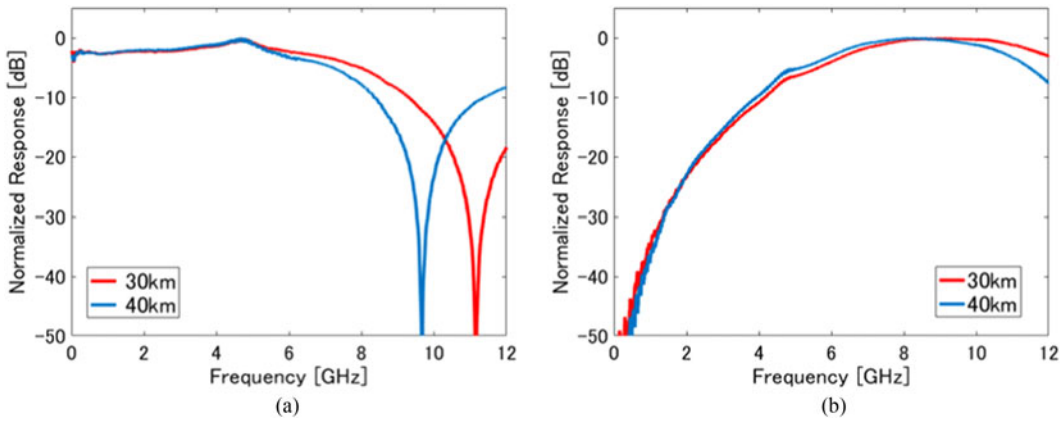

Fig. 5. Measured frequency responses. (a) and (b) IM and PM response, respectively. Red curves represent 30-km transmission and blue ones 40-km transmission.

6.7 and 5.5 GHz, respectively. On the other hand, the 3-dB bandwidths of PM for 30-km and 40-km were 6-11 and 6.4-12 GHz, respectively. From these results, we decided to assign ten f-OFDM signals to both IM and PM. For the IM band, the frequency range of the 10 f-OFDM signals was from 400 MHz to 4 GHz. On the other hand, for the PM band, the frequency range of the other 10 f-OFMD signals was from 6.5 to 10.1 GHz. Therefore, the gap between IM and PM was about 2.5 GHz. As described in Section III, this gap is not always necessary, and we can assign more IF signals. However, in this experiment, we observed the saturation of the RF amplifiers we used due to the high input power. To reduce it, we intentionally set the guard band. These signals were

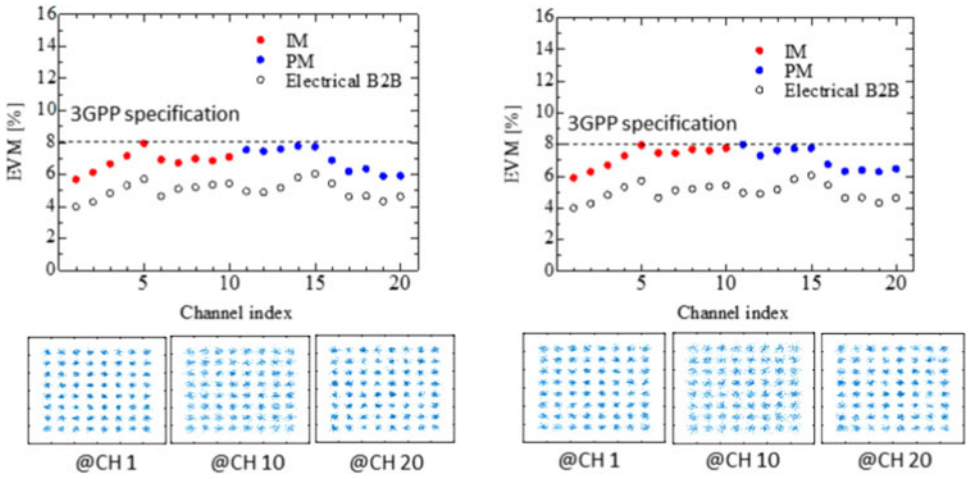

Fig. 6. Measured EVM performances with constellation diagrams at channel 1, 10 and 20. (a) Case after 30-km transmission and (b) after 40-km transmission.

sent to three arbitrary waveform generators (AWGs). To generate 20 IF channels, we used 4 output ports of 3 AWGs and assigned them equally. Thus, each port generated 5 channels.

The output from a laser diode (LD) at 1550 nm was split into two branches by using a 3-dB coupler; One for IM and the other for PM. The linewidth of the laser was $<$100 kHz. Large laser phase noise is also expected to be converted to intensity fluctuation together with the PM signal due to the PM-IM conversion. However, according to the analysis in [21], such noise becomes a critical issue when the linewidth of the laser and the accumulated chromatic dispersion exceed several tens of MHz and several thousand picoseconds per nanometers, respectively. Thus, we do not have to consider the effect of laser linewidth in this experiment. Polarization controllers (PCs) were used to adjust the state of polarization (SOP) at each branch. The electrical signals generated by AWGs were amplified before driving IM and PM. The spectrum of the signal before driving IM and PM is shown in Fig. 4(a) and (b), respectively. The output optical powers from IM and PM were set to be the same to obtain the same performances. The root-mean-square (RMS) optical modulation index of IM was about 10%. Two modulated optical signals were multiplexed by a PBC and transmitted with a launched power of 3 dBm. After transmission, the optical signal was pre-amplified by an erbium doped fiber amplifier (EDFA). We observed the saturation of PD when the optical received power exceeded 1.5 dBm; thus, we set it at 1.5 dBm using a variable optical attenuator (VOA). The optical signal was detected by a PD and the output electrical signal was sampled by an 80-Gsample/s digital oscilloscope. The RF spectra of the received electrical signal after 30-km and 40-km transmission are shown in Fig. 4(c1) and (c2), respectively. Through off-line digital signal processing (DSP), each IF signal was downconverted to the baseband and passed through the matched filter. After synchronization and removing the CP, FFT was performed to demodulate the 64-QAM signals. Finally, the EVM values were measured for all channels.

The measured EVM performances are plotted in Fig. 6(a) and (b). EVMs in the electrical back-to-back condition are represented by open circles as a reference. The red and blue dots show EVMs of signals generated from IM and PM, respectively with constellation diagrams at channels 1, 10 and 20. We confirmed that the EVM performances after 30-km and 40-km transmission degrade by about 2% compared to the electrical back-to-back case due to optical transmission. However, we also confirmed that all the values satisfy the 8%-threshold for 64-QAM that is specified in 3GPP requirements. If this signal is transmitted by CPRI, the data rate becomes 20 (IF channel) $\times$ 2 (IQ) $\times$ 614.4 MHz (sampling rate) $\times$ 16 (resolution) $\times$ 16/15 (CPRI overhead) $\times$ 10/8 (8b/10b encoding) $=$ 524.28 Gbps.

5. Conclusion

We have demonstrated a broadband IFoF transmission scheme utilizing an IM/PM parallel transmitter with appropriate bandwidth allocations to IM and PM. Thanks to the proposed scheme, we could avoid all the null frequencies caused by dispersion-induced RF power fading. As a result, we could increase the available bandwidth significantly. Also, the proposed system was less complicated than the conventional parallel transmitter since it did not require any synchronization between IM and PM. In addition, we could make this system highly flexible (i.e., no significant dependence on transmission distance) by automatically deciding the bandwidth allocations. In a series of demonstrations, we successfully transmitted 20 $\times$ 360-MHz f-OFDM signals, corresponding to a CPRI-equivalent data rate of 524.28 Gbps, over a 30-km and 40-km SMF using the proposed technique. The results showed that the EVM values of all the subcarriers satisfied the 8% threshold for both transmission distances. Thus, we believe that the proposed IFoF transmission system is applicable to long-distance mobile fronthaul links for the 5G wireless systems and beyond.

References

[1] K. Tanaka and A. Agata, "Next-generation optical access networks for C-RAN," in *Proc. Opt. Fiber Commun. Conf.*, 2015, Paper Tu2E.1.
[2] CPRI specification v7.0, 2015.
[3] 3GPP TR 38.801 v2.0.0 Release 14, 2017.
[4] L. Valcarenghi, K. Kondepu, F. Giannone, and P. Castoldi, "Requirements for 5G fronthaul," in *Proc. Int. Conf. Transparent Opt. Netw.*, 2016, Paper We.C2.1.
[5] X. Liu, H. Zeng, N. Chand, and F. Effenberger, "Experimental demonstration of high-throughput low-latency mobile fronthaul supporting 48 20-MHz LTE signals with 59-Gb/s CPRI-equivalent rate and 2-ms processing latency," in *Proc. Eur. Conf. Opt. Commun.*, 2015, Paper We.4.4.3.
[6] L. Cheng, X. Liu, N. Chard, F. Effenberger, and G. Chang, "Experimental demonstration of sub-Nyquist sampling for bandwidth- and hardware-efficient mobile fronthaul supporting 128 $\times$ 128 MIMO with 100-MHz OFDM signals," in *Proc. Opt. Fiber Commun. Conf.*, 2015, Paper W3C.3.
[7] X. Liu, H. Zeng, N. Chand, and F. Effenberger, "Efficient mobile fronthaul via DSP-based channel aggregation," *J. Lightw. Technol.*, vol. 34, no. 6, pp. 1556–1564, Mar. 2016.
[8] J. Capmany and D. Novak, "Microwave photonics combines two worlds," *Nature Photon.*, vol. 1, pp. 319–330, 2007.
[9] D. F. Hewitt, "Orthogonal frequency division multiplexing using baseband optical single sideband for simpler adaptive dispersion compensation," in *Proc. Opt. Fiber Commun. Conf.*, 2007, Paper OME7.
[10] M. Schuster *et al.*, "Spectrally efficient compatible single-sideband modulation for OFDM transmission with direct detection," *IEEE Photon. Technol. Lett.*, vol. 20, no. 9, pp. 670–672, May 2008.
[11] J. Park, W. V. Sorin, and K. Y. Lau, "Elimination of the fibre chromatic dispersion penalty on 1550 nm millimeter-wave optical transmission," *Electron. Lett.*, vol. 33, pp. 512–513, 1997.
[12] Y. Gao, A. Wen, L. Liu, S. Tian, S. Xiang, and Y. Wang, "Compensation of the dispersion-induced power fading in an analog photonic link based on PM-IM conversion in a Sagnac loop," *J. Lightw. Technol.* vol. 33, no. 13, pp. 2899–2904, Jul. 2015.
[13] V. J. Urick and F. Bucholtz, "Modulation diversity for chromatic dispersion compensation in analog photonic links," Naval Res. Lab., Washington, DC, USA, NRL Memorandum Report, NRL/MR/5650-06-8977, 2006.
[14] Y. Cui *et al.*, "Overcoming chromatic-dispersion-induced power fading in ROF links employing parallel modulators," *IEEE Photon. Technol. Lett.*, vol. 24, no. 14, pp. 1173–1175, Jul. 2012.
[15] S. Ishimura *et al.*, Simultaneous transmission of aggregated microwave and millimeter-wave signals over fiber with parallel IM/PM transmitter for mobile fronthaul links, in *Proc. Eur. Conf. Opt. Commun.*, 2017, Paper Tu.1.B.1.
[16] 3GPP TS 36.104 v12.5.0 Release 12, 2014.
[17] G. J. Meslener, "Chromatic dispersion induced distortion of modulated monochromatic light employing direct detection," *IEEE J. Quantum Electron.*, vol. QE-20, no. 10, pp. 1208–1216, Oct. 1984.
[18] H. Chi, X. Zou, and J. Yao, "Analytical models for phase-modulation-based microwave photonic systems with phase modulation to intensity modulation conversion using a dispersive device," *J. Lightw. Technol.*, vol. 27, no. 5, pp. 511–521, Mar. 2009.
[19] China Mobile Research Institute, Alcatel-Lucent, Nokia Networks, ZTE Corporation, Broadcom Corporation and Intel China Research Center, "White paper of next generation fronthaul interface," 2015.
[20] X. Zhang, M. Jiay, L. Chen, J. May, and J. Qiu, "Filtered-OFDM—Enabler for flexible waveform in the 5th generation cellular networks," in *Proc. IEEE Conf. Global Commun.*, 2015, pp. 1–6.
[21] S. Yamamoto, N. Edagawa, H. Taga, Y. Yoshida, and H. Wakabayashi, "Analysis of laser phase noise to intensity noise conversion by chromatic dispersion in intensity modulation and direct detection optical-fiber transmission," *J. Lightw. Technol.*, vol. 8, no. 11, pp. 1716–1722, Nov. 1990.